Structures and Topological Transitions of Hydrocarbon Films on Quasicrystalline Surfaces

Wahyu Setyawan,[1] Renee D. Diehl,[2] and Stefano Curtarolo[1,*]

[1]*Department of Mechanical Engineering and Materials Science, Duke University, Durham, North Carolina 27708, USA*
[2]*Department of Physics and Materials Research Institute, Penn State University, University Park, Pennsylvania 16802, USA*

(Received 5 December 2008; published 3 February 2009)

Lubricants can affect quasicrystalline coating surfaces by modifying the commensurability of the interfaces. We report results of the first computer simulation studies of physically adsorbed hydrocarbons on a quasicrystalline surface: methane, propane, and benzene on decagonal Al-Ni-Co. The grand canonical Monte Carlo method is employed, using novel embedded-atom method potentials generated from *ab initio* calculations, and standard hydrocarbon interactions. The resulting adsorption isotherms and calculated structures show the films' evolution from submonolayer to condensation. We discover the presence and absence of the fivefold to sixfold topological transition, for benzene and methane, respectively, in agreement with a previously formulated phenomenological rule based on adsorbate-substrate size mismatch.

DOI: 10.1103/PhysRevLett.102.055501 PACS numbers: 61.44.Br, 68.43.Hn, 68.55.A−

Friction can become vanishingly small between incommensurate interfaces (superlubricity) [1,2]. The aperiodic structure of quasicrystal (QC) surfaces makes them the ideal candidates for this phenomenon. Indeed, the special frictional properties of QCs have been confirmed in a series of experiments using atomic force microscopy on single grain QCs [3–8]. Although its origin is not yet completely understood, the evidence suggests that poor coupling of phonons at the interfaces may play a major role [6–8]. There is also evidence that oxidation decreases the friction even further [4,9]. In fact, even before these single crystal experiments were performed, experiments on QC coatings in air did show low-friction behavior [10], leading to applications involving moving machine parts and nonstick cookware [11].

Since the low friction of QCs is clearly related to their structure, the interaction of the lubricant with the QC and the structure of the lubricating film is particularly important. In most applications involving machine parts, additional lubricant would be needed to address the frictional contributions of grain boundaries and asperities. Studies of metal and rare gas adsorption on QCs indicate that both periodic and aperiodic structures can occur in thin films [12–17]. However, little is known about the interaction of hydrocarbons with QC surfaces [5,18,19].

In this Letter, we explore the effect of structural and symmetry mismatches on the ordering of hydrocarbons by evaluating the nature of hydrocarbon adsorption (methane, propane, and benzene) on a quasicrystalline decagonal surface, namely, the tenfold surface of $Al_{73}Ni_{10}Co_{17}$. The simulations are performed using the grand canonical Monte Carlo method, with which we have extensive experience on smooth [20–22] and corrugated substrates [15–17,23–25]. Using the grand canonical Monte Carlo method, we compute the adsorption properties for specified thermodynamic conditions. We take a tetragonal unit cell, of side 5.12 nm, with a hard wall at 10 nm above the surface to confine the coexisting vapor phase without causing capillary condensation (sufficient to contain 25 layers of benzene). We assume periodic boundary conditions which, although sacrificing the accuracy of the long-range QC structure, do not interfere with short-to-moderate length scales, representative of the hydrocarbon order. The substrate is reproduced with an 8-layer Al-Ni-Co slab, where the atom coordinates are derived from an experimental low-energy electron diffraction study [26]. The intermolecular interactions (adsorbate-adsorbate) are calculated as a sum of pair interactions between atoms. Buckingham potentials are used for methane [27,28] and benzene [29,30], while a Morse potential is employed for propane [31]. We have developed embedded-atom method (EAM) potentials [32] to model the many-body intramolecular interactions, adsorbate-substrate (C-Al, C-Co, C-Ni, H-Al, H-Co, H-Ni) and substrate-substrate (Al-Al, Al-Co, Al-Ni, Co-Co, Co-Ni, Ni-Ni). The EAM embedding functions are taken as natural cubic splines using charge density functionals from Herman [33], while the EAM pair energies have Morse potential forms [34] with Haftel's mixing scheme [35], if necessary. The EAM potential parameters are fitted from *ab initio* energies calculated using the Vienna *ab initio* simulation package (VASP) [36] with exchange-correlation functionals as parametrized by Perdew, Burke, and Ernzerhof [37] for the generalized gradient approximation, and projector augmented-wave [38] pseudopotentials. The EAM potential parameters, fitted using the simplex method [39], are summarized in the EPAPS material [40]. QC approximants (periodic crystals having similar short-range order) are used to address the periodic boundary conditions required by the *ab initio* package: we use $Al_{29}Co_4Ni_8$, $Al_{17}Co_5Ni_3$, and $Al_{34}Co_4Ni_{12}$ [41]. Our calculations show that alkanes and benzene do not dissociate on such substrates, which do not undergo any considerable relaxation upon the adsorption of the molecules. Thus, the substrate and the molecules can

be approximated as rigid, although the molecules are allowed to explore all rotational degrees of freedom [42].

The adsorption potential of one molecule, $V_{\min}(x, y)$, calculated as the maximum depth as a function of normal z-coordinate and Euler angles (θ, ϕ, ψ), is deep and highly corrugated. Figure 1 shows $V_{\min}(x, y)$ for methane and benzene: the dark spots indicate strong binding sites. The average adsorption energy is 221 meV/methane, 374 meV/propane, and 931 meV/benzene.

The symmetry of the adsorption potentials for methane and benzene reflect the pentagonal symmetry of the substrate, as illustrated in Fig. 1. Propane follows a similar trend as methane, with somewhat less corrugation due to its larger size. The most attractive adsorption positions for methane and propane [40] are located at the centers of pentagonal hollows having five Al atoms at the vertices. Conversely, the most attractive sites for benzene are the Al-centered pentagons with 3 Al and 2 Ni atoms at the vertices. These hollow and Al-centered pentagons alternate every 36° around the z axis.

By simulating the adsorption of one molecule, a general trend is observed for the orientation of the adsorbent: the smaller the molecule, the more variation in the rotation of the ground state. Methane's ground state is highly degenerate; propane adsorbs with its axis forming a small angle with respect to the substrate (the angle varies from 0° to 10° depending on the adsorption site). Benzene adsorbs with its plane parallel to the substrate.

Figure 2 shows the computed adsorption isotherms ρ_N (densities in molecules/nm^2) at different temperatures for methane (T = 68, 85, 136, 185 K), propane (T = 80, 127, 245, 365 K), and benzene (T = 209, 270, 418, 555 K) as functions of pressure P. The plotted quantities are the thermodynamic excess coverages (differences between the total number of molecules and the number that would be present if the cell were filled with uniform vapor). The substrate is very attractive (Fig. 1); hence, the hydrocarbons experience complete wetting up to the highest temperature close to the critical temperature. At low temperatures, the formation of the first layers is evident from the first step in each plot (the most left isotherms). The formation of further layers is not clearly observed, in contrast with the observations for noble gases [15–17,24]. Nevertheless, layering in the adsorbed film is revealed by the insets of Fig. 2, showing the adsorption densities along the z direction at the pressures corresponding to points d of the lowest temperature isotherms. The relative positions of z_1, z_2, and z_3 indicate that methane adsorbs mostly with three hydrogens anchored to the QC, while propane adsorbs mostly with five hydrogens near the QC (two from each end and one from the middle segment).

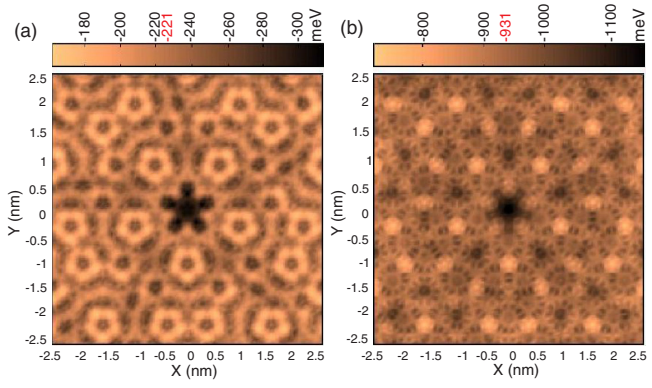

FIG. 1 (color online). Computed potential energies for (a) methane and (b) benzene on Al-Ni-Co, obtained by minimizing $V(x, y, z, \theta, \phi, \psi)$ of a single molecule with respect to (z, ψ, θ, ϕ) variations. The average values are 221 meV/methane and 931 meV/benzene.

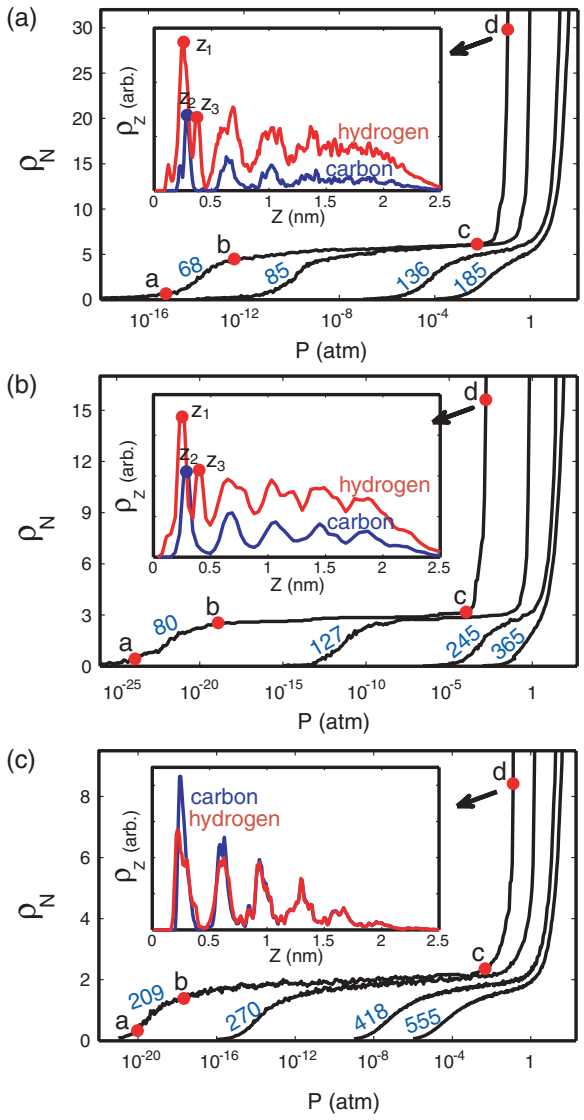

FIG. 2 (color online). Isothermal adsorption densities (ρ_N in molecules/nm^2) of (a) methane (T = 68, 85, 136, 185 K), (b) propane (T = 80, 127, 245, 365 K), and (c) benzene (T = 209, 270, 418, 555 K) on decagonal Al-Ni-Co. The insets represent the densities along the z direction at P corresponding to points d.

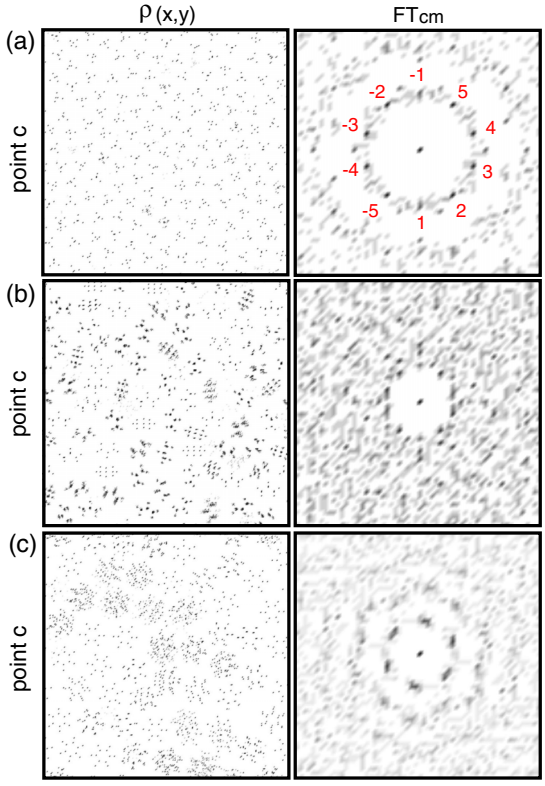

FIG. 3 (color online). Monolayer density profiles $\rho(x, y)$ and Fourier transforms of the density of the center of mass FT_{cm} for (a) methane at 68 K [point c in Fig. 2(a)], (b) propane at 80 K [point c in Fig. 2(b)], and (c) benzene at 209 K (point c in Fig. 2(c)] adsorbed on decagonal Al-Ni-Co.

In the submonolayer regime [point a in Fig. 2(a)], methane adsorbs preferentially at the strong binding sites. By increasing P, a methane monolayer forms with pentagonal ordering commensurate with the substrate [point c in Fig. 2(a)]. Similar configurations are observed at all studied temperatures. An example of such ordering is illustrated in Fig. 3(a) at $T = 68$ K: the density profile $\rho(x, y)$ and the Fourier transform FT_{cm} of the density of the center of mass confirm pentagonal ordering (10 discrete spots representing fivefold axes in FT_{cm}). Similar plots for propane at 80 K and benzene at 209 K are shown in Figs. 3(b) and 3(c), respectively. At all simulated temperatures, benzene has sixfold order as indicated by its FT_{cm} characteristic of triangular lattice. Unlike methane and benzene, which adsorb in a well-defined structure, propane forms a poorly ordered fivefold arrangement (clusters of molecules which form pentagons can be seen in the EPAPS material [40]). The FT_{cm} indicates a distortion involving a compression along one direction. This is due to the interplay between the linear form of the propane molecule and the QC structure. Figure 4 shows a histogram of the orientations of the propane's axis projected on the xy plane [panel (a)] and the xz plane [panel (b)], corresponding to the density plot in Fig. 3(b). Indeed, propane adsorbs with its axis parallel with the substrate (up to 10°) and preferentially oriented along the x axis.

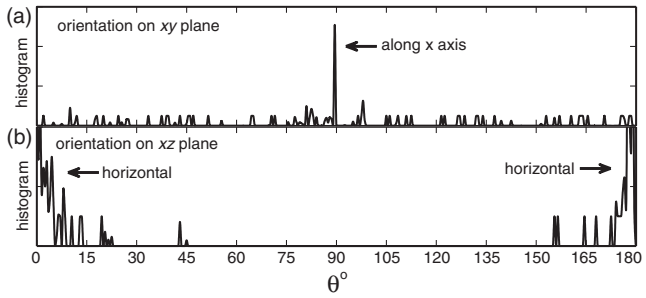

FIG. 4. Histogram of orientation of propane's axis on (a) xy plane and (b) xz plane at monolayer coverage at 80 K adsorbed on decagonal Al-Ni-Co. The corresponding density plot is depicted in Fig. 3(b).

Figure 5(a) illustrates a superposition of the methane monolayer at 85 K and the top layer of substrate atoms. Methane molecules are present in every hollow pentagon defined by five Al atoms. These pentagons, corresponding to the dominant binding sites and depicted as dark spots in Fig. 1(a), are responsible for stabilizing the quasicrystalline structure of the methane monolayer. A similar plot for benzene at 209 K is given in Fig. 5(b). A domain having sixfold order can be observed in the left part of the figure. Dashed circles corresponding to the benzene molecules are drawn to illustrate the orientation of this domain, which makes an angle of 18° from the y axis. Thus, the benzene lattice is oriented along a symmetry direction of the QC, as observed previously for the Xe monolayer.

Previously, by studying the adsorbed monolayer of rare gases [16,17], we found that the crucial parameter in determining the overlayer structure is the relative size mismatch between the adsorbate's and substrate's characteristic length. The mismatch is defined as $\delta_m \equiv (d_r - \lambda_r)/\lambda_r$ where d_r is the distance between rows in a two-dimensional close-packed arrangement of adsorbates [17,43], and $\lambda_r = 0.381$ nm is the QC's characteristic length [14]. Thus, δ_m measures the relative mismatch between an adsorbed {111} closed-packed plane of adsorbates and the QC surface. The proposed rule states that the

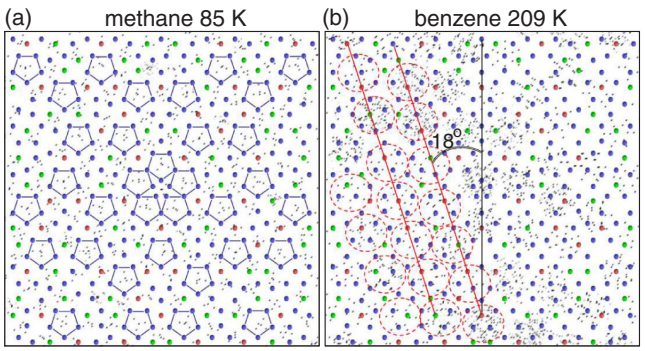

FIG. 5 (color online). (a) Methane monolayer at 85 K and (b) benzene monolayer at 209 K adsorbed on decagonal Al-Ni-Co. The top layer of substrate atoms is plotted in blue (Al), green (Ni), and red (Co).

TABLE I. Summary of adsorbed rare gases and selected hydrocarbons undergoing (or not) the commensurate → incommensurate transition on Al-Ni-Co. *i*Ne, *i*Xe, and *d*Xe are inflated/deflated noble gases [17]. Triangles and pentagons indicate triangular lattice and fivefold structure, respectively.

	δ_m	Transition	Monolayer
Methane	−0.055	No	⬠
Benzene	0.617	Yes	△
Xe [15,16]	0.016	Yes	△
Ne [17]	−0.311	No	△ + ⬠
Ar [17]	−0.158	No	△ + ⬠
Kr [17]	−0.108	No	△ + ⬠
$i\mathrm{Ne}^{(1)}$ [17]	0.016	Yes	△
$d\mathrm{Xe}^{(1)}$, $d\mathrm{Xe}^{(2)}$ [17]	−0.311, −0.034	No	△ + ⬠
$i\mathrm{Xe}^{(1)}$, $i\mathrm{Xe}^{(2)}$ [17]	0.363, 0.672	Yes	△

ordering transition exists if and only if $\delta_m > 0$ [17]. For methane, by starting from the lattice parameter of the cubic cell [45,46], we have $\delta_m(\mathrm{CH_3}) \sim -0.055$. For benzene, by using d_r obtained from the simulation of the sixfold phase (using a flat substrate with the well depth of 931 meV), we get $\delta_m(\mathrm{C_6H_6}) \sim 0.617$. Both methane and benzene satisfy the mismatch rule, extending its applicability (the transition cannot be defined for propane since it does not form pentagonal or triangular arrangements).

Table I summarizes the results obtained for all hydrocarbons and rare gases that we have studied so far. When the transition is not present, the monolayer does not form a structure having long-range periodic order. From the point of view of the potential for superlubricity, all of the gases that are smaller than Xe do not form periodic films. In addition, the linear molecule propane, which is larger than Xe, does not. This suggests that the shape as well as the size is an important factor in the ordering, and it may bode well for the use of linear hydrocarbons as lubricants on quasicyrstalline films.

Research was supported by the NSF (DMR-0505160, DMR-0639822) and ACS (Nos. PRF-45814-G5 and PRF-48661-AC5). We thank the Teragrid Partnership (Texas Advanced Computing Center) for computational support (MCA-07S005).

*Corresponding author.
stefano@duke.edu

[1] M. Hirano and K. Shinjo, Phys. Rev. B **41**, 11 837 (1990).
[2] M. Dienwiebel *et al.*, Phys. Rev. Lett. **92**, 126101 (2004).
[3] J. Y. Park *et al.*, Tribol. Lett. **17**, 629 (2004).
[4] J. Y. Park *et al.*, Science **309**, 1354 (2005).
[5] J. Y. Park *et al.*, Phys. Rev. B **71**, 144203 (2005).
[6] J. Y. Park *et al.*, Phys. Rev. B **74**, 024203 (2006).
[7] J. Y. Park *et al.*, Philos. Mag. **86**, 945 (2006).
[8] J. Y. Park *et al.*, J. Phys. Condens. Matter **20**, 314 012 (2008).
[9] J. M. Dubois *et al.*, Philos. Mag. **86**, 797 (2006).
[10] J. M. Dubois, S. S. Kang, and J. Von Stebut, J. Mater. Sci. Lett. **10**, 537 (1991).
[11] J. M. Dubois, *Useful Quasicrystals* (World Scientific, Singapore, 2003).
[12] V. Fournée and P. A. Thiel, J. Phys. D **38**, R83 (2005).
[13] H. R. Sharma, M. Shimoda, and A. P. Tsai, Adv. Phys. **56**, 403 (2007).
[14] N. Ferralis *et al.*, Phys. Rev. B **69**, 075410 (2004).
[15] S. Curtarolo *et al.*, Phys. Rev. Lett. **95**, 136104 (2005).
[16] W. Setyawan *et al.*, Phys. Rev. B **74**, 125425 (2006).
[17] W. Setyawan *et al.*, J. Phys. Condens. Matter **19**, 016 007 (2007).
[18] J. T. Hoeft *et al.*, Philos. Mag. **86**, 869 (2006).
[19] R. McGrath *et al.*, J. Alloys Compd. **342**, 432 (2002).
[20] F. Ancilotto *et al.*, Phys. Rev. Lett. **87**, 206103 (2001).
[21] S. Curtarolo *et al.*, Phys. Rev. E **59**, 4402 (1999).
[22] M. J. Bojan *et al.*, Phys. Rev. E **59**, 864 (1999).
[23] S. Curtarolo *et al.*, Phys. Rev. E **59**, 4402 (1999).
[24] R. D. Diehl *et al.*, Philos. Mag. **87**, 2973 (2007); **86**, 863 (2006).
[25] R. D. Diehl, W. Setyawan, and S. Curtarolo, J. Phys. Condens. Matter **20**, 314 007 (2008).
[26] N. Ferralis *et al.*, Phys. Rev. B **69**, 153404 (2004).
[27] S. Tsuzuki, T. Uchimaru, and K. Tanabe, J. Mol. Struct. **99**, 273 (1993).
[28] S. Tsuzuki *et al.*, J. Phys. Chem. **98**, 1830 (1994).
[29] S. Califano, R. Righini, and S. H. Walmsley, Chem. Phys. Lett. **64**, 491 (1979).
[30] R. Chelli *et al.*, Phys. Chem. Chem. Phys. **3**, 2803 (2001).
[31] J.-P. Jalkanen *et al.*, J. Chem. Phys. **116**, 1303 (2002).
[32] M. S. Daw and M. I. Baskes, Phys. Rev. Lett. **50**, 1285 (1983).
[33] A. Herman, Int. J. Nanotechnology **2**, 215 (2005).
[34] P. M. Morse, Phys. Rev. **34**, 57 (1929).
[35] M. I. Haftel, Phys. Rev. B **48**, 2611 (1993).
[36] G. Kresse and J. Hafner, Phys. Rev. B **47**, 558 (1993).
[37] J. P. Perdew, K. Burke, and M. Ernzerhof, Phys. Rev. Lett. **77**, 3865 (1996).
[38] P. E. Blöchl, Phys. Rev. B **50**, 17 953 (1994).
[39] J. A. Nelder and R. Mead, Computer Journal **7**, 308 (1965).
[40] See EPAPS Document No. E-PRLTAO-102-028907 for the EAM potentials parametrizations and additional plots. For more information on EPAPS, see http://www.aip.org/pubservs/epaps.html.
[41] Database of alloys, M. Widom and M. Mihalkovic, http://alloy.phys.cmu.edu/.
[42] Even though the substrate is rigid, it experiences different charge density in different grand canonical Monte Carlo configurations; therefore, the embedding energy needs to be updated in each step.
[43] For adsorbates described by Lennard-Jones interactions $d_r = k \cdot \sigma_{gg}$, where $k = 0.944$ is the distance between rows in a close-packed plane of a bulk Lennard-Jones gas with $\sigma = 1$ at $T = 0$ K [44], and σ_{gg} is the Lennard-Jones size parameter of the gas-gas potential.
[44] L. W. Bruch, P. I. Cohen, and M. B. Webb, Surf. Sci. **59**, 1 (1976).
[45] H. H. Mooy, Nature (London) **127**, 707 (1931).
[46] H. M. James and T. A. Keenan, J. Chem. Phys. **31**, 12 (1959).